



Suppression of Sclerostin Alleviates Radiation Damage to Bone by Protecting Bone forming Cells

Abhishek Chandra¹

Tiao Lin¹

Wei-ju Tseng¹

Keith Cengel²

Michael A. Levine³

X. Sherry Liu¹

Ling Qin¹

¹Departments of Orthopaedic Surgery

²Radiation Oncology
Perelman School of Medicine
University of Pennsylvania
Philadelphia, Pennsylvania

³Division of Endocrinology and Center for
Bone Health Diseases
The Children's Hospital of Philadelphia.

Introduction:

Radiation damage to the skeleton within the radiation field results in a spectrum of bone changes from mild osteopenia to osteoradionecrosis.¹ We have demonstrated that radiation markedly suppressed bone turnover and that bone tissue atrophy is the most common outcome after radiation. We hypothesize that functional recovery of bone architecture in this adverse environment will be possible by the use of anabolic bone forming agents. As a proof of principle, we showed that recombinant human parathyroid hormone (rhPTH1-34, teriparatide), the only FDA-approved anabolic treatment for osteoporosis, completely abrogated the damaging effects of radiation in rat bones.² Due to a tumorigenic concern with the use of PTH during radiotherapy, an alternative was sought after. Mechanistic studies revealed that Wnt pathway played an essential role in teriparatide function in protecting bone against radiation. Sclerostin is a Wnt antagonist which binds with the Wnt co-receptor LRP5/6 and its expression in adults is largely restricted in osteocytes. Loss of Sclerostin function in human patients, as in the case of sclerosteosis and van Buchem disease, or in *SOST* knockout mice, result in high bone mass phenotype with no increased tumor formation. Therefore, we hypothesize that suppression of Sclerostin renders structural and functional protection to the radiated bones, while minimizing the potential risks.

Methods:

Small animal radiation research platform (SARRP) radiation and Scl-Ab treatment- All procedures were approved by our institution's Animal Care and Use Committee. Sclerostin antibody (Scl-Ab) and *SOST* knockout (KO) mice were provided by Novartis pharmaceuticals. Two-month-old male *WT* (C57BL6) mice and *SOST*-KO mice received two 8 Gy doses delivered on days 1 and 3 to the distal metaphyseal region of the right femurs from SARRP (Xstrahl), a clinically relevant focal irradiator for rodents. This was designed to mimic the typical femur dose constraints for whole pelvis intensity modulated radiotherapy for patients with prostate, rectal, or endometrial cancers. Following radiation, *WT* mice were subcutaneously injected with either vehicle or Scl-Ab (100 mg/kg/week) for 4 weeks.

On day 28, bilateral femurs (radiated and non-radiated) were harvested for μ CT, histology, and histomorphometry, and serum were collected for bone markers. For dynamic labeling, calcein (15 mg/kg) and xylenol orange (90 mg/kg) were injected at 9 and 2 days, respectively, before euthanization. *μ CT and finite element analysis (FEA)*- The metaphysis of distal femur was scanned by μ CT 35 (Scanco Medical AG) at 6 μ m resolution followed by calculation of trabecular bone structural parameters and stiffness (n = 7/group). *Histomorphometry*- After μ CT scanning, femurs were processed for plastic embedding for static and dynamic histomorphometric analysis. Osteocyte (Ocy.) and adipocyte (Ad.) number were also quantified. *Histology*- At 2 weeks post radiation, femurs (n = 5/group) were harvested for paraffin embedding followed by TUNEL staining (Apoptag[®] TM, Millipore). At 1 week post radiation, femurs were processed for frozen embedding followed by Alexa-488-labeled phalloidin staining to visualize F-actin fibers. *Colony Forming Assay*- Two month old *WT* mice (n = 3/group) and *SOST*-KO mice (n = 3) were radiated and injected with Scl-Ab as described above. At 2 weeks, femurs were harvested, cleaned and the metaphyseal bones were digested with collagenase. Cells were seeded at 1×10^6 /T25 flask in the growth medium for CFU-F assay. *Statistics*- Data are expressed as means \pm SEM and analyzed by paired, two-tailed Student's t-test for comparison of radiated and non-radiated legs and by unpaired, two-tailed Student's t-test for comparison of vehicle and Scl-Ab-treated samples and for comparison of *WT* and *SOST*-KO samples.

Results:

Focally irradiated adult mice at distal femoral metaphysis that received 16 Gy radiation generated from SARRP induced a significant trabecular bone loss and structural deterioration in irradiated femurs compared to contralateral ones in vehicle-treated mice (BMD: -20%; BV/TV: -21%; Tb.N: -10%; SMI: +30%; Stiffness: -75%) (Figure 1). Remarkably, Scl-Ab injections increased trabecular BMD, BV/TV, Tb.N, decreased SMI and increased stiffness to a similar level regardless of radiation, implying that Scl-Ab treatment is able to reverse radiation-induced bone damage in a clinical setting. Interestingly, *SOST*-KO mice were markedly resistant against any structural damage

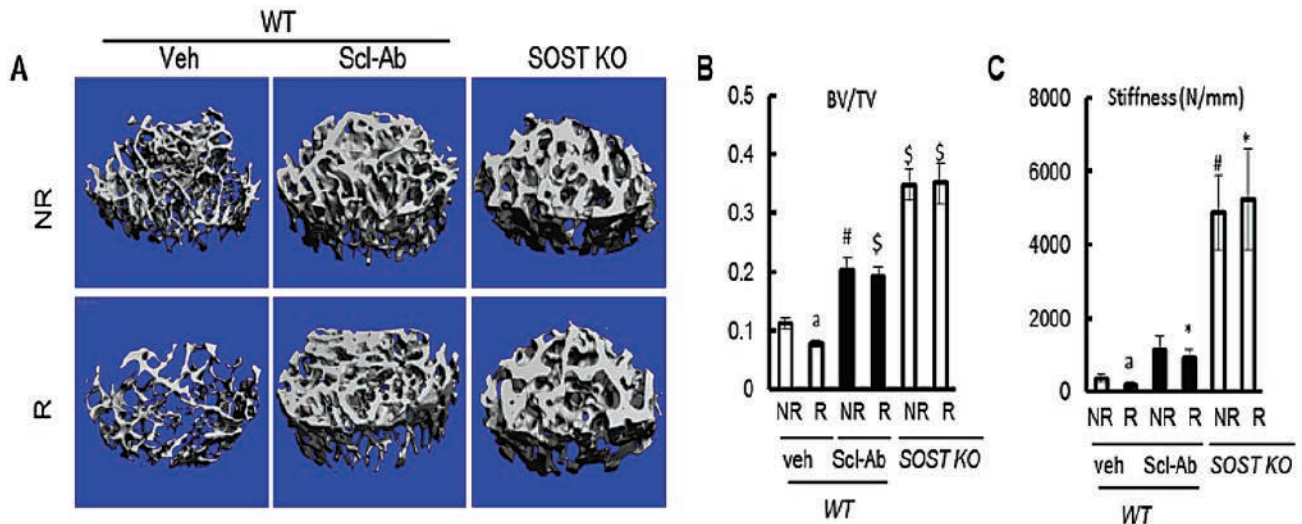


Figure 1. Suppression of Sclerostin greatly improves bone turnover of radiated bones. A. 3-D μ CT images at 6 μ m resolution, revealing the trabecular architecture. B. Bone volume fraction as a ratio of total volume. a; $p < 0.05$ NR vs R. #; $p < 0.01$ vs veh-NR, \$; $p < 0.01$ vs veh-R. C. Finite element analysis, a; $p < 0.05$ NR vs R. #; $p < 0.01$ vs veh-NR, *; $p < 0.01$ vs veh-R.

from ionizing radiation. Static histomorphometry indicated that radiation negatively regulated the bone forming cells (Ob.N: -30%, Ocy.N.: -33%, empty Ocy.lacunae: +6-fold, Ad.N.: +10-fold). Dynamic histomorphometry revealed a 10-fold suppression in active bone formation post-irradiation. TUNEL staining revealed a 4-fold increase in apoptotic osteoblasts in the radiated bones. Amazingly, suppression of *SOST* not only protected the osteoblasts, but also partially but significantly suppressed the adipocyte formation after radiation. As compared to the 10-fold reduction in the control, Scl-Ab had a significantly higher bone formation rate, which was correlated by an overall increase in serum osteocalcin levels in the Scl-Ab treated animals. To assess the early stage effect of radiation on osteocytes, F-actin staining revealed a shortening of canaliculae, leading to impaired osteocytic connections with the bone surface and neighboring osteocytes (Figure 2). In contrast, Scl-Ab treatment, not only improved the length of canaliculae, but also protected the inter-osteocytic connections, which is considered important for the overall bone turnover and health. In bone, osteoblasts and osteocytes are derived from bone marrow mesenchymal progenitors (MP's). CFU-F assay clearly revealed that, while radiation greatly diminished the progenitor numbers (-90%), Scl-Ab treatment significantly increased these progenitor numbers by 2-fold.

Discussion:

This study provides proof-of-principle that Scl-Ab blocks bone loss and microarchitecture deterioration after radiation. Furthermore Scl-Ab not only protects the bone forming cells, including MP's, osteoblasts and osteocytes from cell death, but also inhibits the differentiation of MP's towards adipocytes on exposure to radiotherapy.

Conclusions

Scl-Ab treatment minimizes or fully rescues bone loss and damage associated with radiotherapy, and therefore provides

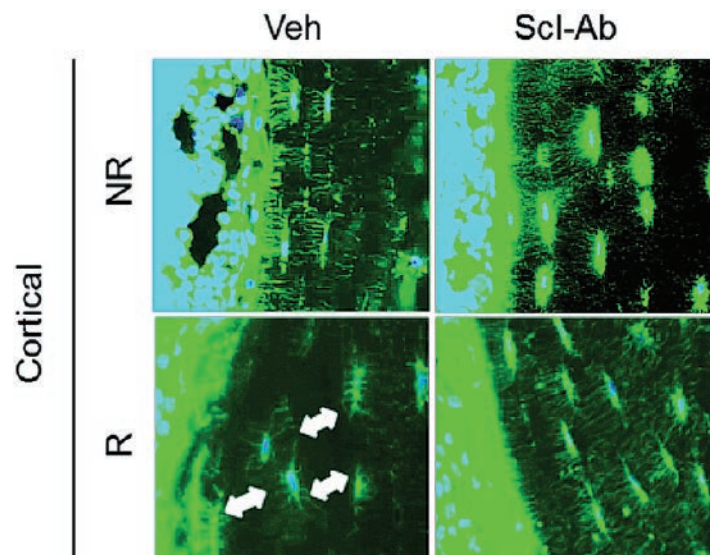


Figure 2. Scl-Ab protects the osteocyte canicular-network from ionizing radiation. Double headed arrows indicate the lack of canalicular connections.

a potential therapeutic treatment for radiation induced osteoporosis.

Acknowledgements

This work was supported by the National Institute of Health (R01DK095803 to LQ), Penn Center for Musculoskeletal Disorders P30AR050950 (NIAMS/NIH), ASBMR Junior Faculty Osteoporosis Basic Research Award (to LQ) and McCabe Pilot Award (to XSL).

References:

1. Howland, W.J., *et al.* Postirradiation atrophic changes of bone and related complications. *Radiology* 1975. 117 (3 Pt 1):p. 677-85
2. Chandra, A., *et al.* PTH1-34 Blocks radiation-induced osteoblast apoptosis by enhancing DNA repair through canonical Wnt pathway. *J Biol Chem* 2015. 290(1): p. 157-167.